Robotica (2022), **40**, pp. 279–293
doi:10.1017/S0263574721000527

CAMBRIDGE UNIVERSITY PRESS

RESEARCH ARTICLE

Desired model compensation-based position constrained control of robotic manipulators

Samet Gul[1], Erkan Zergeroglu[1]*, Enver Tatlicioglu[2], and Mesih Veysi Kilinc[3]

[1]Department of Computer Engineering, Gebze Technical University, 41400, Gebze, Kocaeli, Turkey
[2]Department of Electrical & Electronics Engineering, Ege University, 35100, Bornova, Izmir, Turkey
[3]Institute of Information Technologies, Gebze Technical University, 41400, Gebze, Kocaeli, Turkey
*Corresponding author. Email: e.zerger@gtu.edu.tr

Received: 23 April 2020; **Revised:** 11 April 2021; **Accepted:** 12 April 2021; **First published online:** 14 May 2021

Keywords: Robotic manipulators, Position constraint, Full-state feedback, Lyapunov-based approach

Abstract

This work presents the design and the corresponding stability analysis of a desired model-based, joint position constrained, controller formulation for robotic manipulators. Specifically, provided that the initial joint position tracking error signal starts within some predefined region, the proposed controller ensures that the joint tracking error signal remains inside this region and approaches to zero asymptotically. Extensive numerical simulations and experimental studies performed on a two-link direct-drive planar robot are provided in order to illustrate the effectiveness and feasibility of the proposed controller.

1. Introduction

One drawback of controller designs for multi-input multi-output (MIMO) systems based on Lyapunov-type analysis techniques is the lack of direct knowledge of the transient performance of the system states. As the outcome of the stability analysis via Lyapunov-based arguments is usually stated with respect to increasing time. Specifically, when the overall stability result obtained through a Lyapunov-based analysis is asymptotic stability of the system states, we can conclude that the states of the system remain bounded (i.e., in $\mathcal{L}_\infty$) and will eventually converge to the desired states, but this does not give information on how the states behave during the transient. However, on real-world systems, transient behaviour is as important as the type of the stability obtained, as this also frames the steady-state behaviour. When the direct manipulation of transient behaviour is not possible, then at least a reasonable bound should be ensured preferably *a priori*. Special to the robotic manipulators, transient behaviour of the system states, and the overshoot is of critical importance [1]. The upper bound of the state overshoot values are restrictive in most robotic applications when there are humans in the proximity of the operating region.

A possible solution to this problem relies on barrier Lyapunov function (BLF) approach-based designs. Although applying constraints was considered in optimisation field for quite some time, its application to non-linear control field is relatively new and dates back to early 2000s [2, 3]. Some line of the past studies applied BLFs to deal with constraints for systems in the Brunovsky form [2], in strict feedback form [3], in strict feedback form with time-varying output constraints [4] and in pure feedback form [5]. An asymmetric BLF was proposed for systems in pure feedback form under time-varying full-state constraints in ref. [6]. In ref. [7], bounding both the trajectory tracking error and the parameter estimation error vector within user-defined constraint sets have been considered. A constraint-based model predictive controller for the tracking control of mobile manipulation was considered in ref. [8].

One line of research have focused on applying BLF type control designs to mechatronic systems. In ref. [9], a systematic motion controller based on BLF was designed for servo systems. In refs. [10] and [11] used prescribed performance criteria for regulation control of robot manipulators, which are extended to tracking control in refs. [12], [13] and [14]. Hackl and Kennel, in ref. [15], designed a position controller with prescribed performance criteria for robot manipulators when dynamic model is partially known. In ref. [16], a task space regulator guaranteeing prescribed performance was proposed while ref. [17] used BLF-based approach for joint limit avoidance sub-task of redundant robot manipulator control problem. In ref. [18], prescribed performance methods were utilised for referential control of human-like movements of redundant arms. In refs. [19] and [20] considered force/position control of robot manipulators with prescribed performance while guaranteeing contact. In ref. [21] a robust adaptive controller was proposed to deal with the joint level constraints of robotic manipulator via use of BLF and an adaptive neural network controller for robot manipulators using integral BLF was proposed in ref. [22]. Recently, some work on adaptive and robust compensation of parametric uncertainties for robot manipulators based on Fourier series expansion has been proposed in refs. [23] and [24], respectively.

In this work, tracking control of robot manipulators in joint space is aimed. In addition to the joint position tracking objective, ensuring *a priori* limits for the entries of the joint tracking error is aimed as the secondary control objective. The control problem is further complicated due to the presence of parametric uncertainties in the mathematical model of the robot manipulator. To ensure tracking control objective, a non-linear proportional derivative feedback component is designed. To deal with the parametric uncertainties, desired model compensation-based adaptive controller component is proposed as part of the control input. Different from the similar designs in the literature, in a novel approach, the control gain of the tracking error is proposed to be error-dependent and two fundamentally different control gain matrices are designed. To ensure limiting the entries of the tracking error in addition to guaranteeing asymptotic convergence to the origin, two BLFs are introduced. To our best knowledge, the proposed method is the first controller approach that fuses the use of BLF design with the desired model-based compensation procedure. Due to the use of the desired trajectory signal, the proposed controller enables a smoother output compared to its counterparts and is less exposed to sensory noise. Numerical simulation results are shown to be commensurate with the analysis and experimental verifications are presented in order to illustrate the feasibility of the proposed method.

2. Robot model

The mathematical model of an n degree of freedom (dof) revolute joint robot manipulator is presented as [25]

$$M(q)\,\ddot{q} + C(q,\dot{q})\,\dot{q} + G(q) + F_d\dot{q} = \tau \tag{1}$$

in which $q\,(t)$, $\dot{q}\,(t)$, $\ddot{q}\,(t) \in \mathbb{R}^n$ are the vectors for joint positions, velocities and accelerations, respectively, $M\,(q) \in \mathbb{R}^{n\times n}$ is the inertia matrix, $C\,(q,\dot{q}) \in \mathbb{R}^{n\times n}$ is the centripetal Coriolis matrix, $G\,(q) \in \mathbb{R}^n$ represents the gravitational effects, $F_d \in \mathbb{R}^{n\times n}$ is a positive definite diagonal matrix denoting the constant viscous frictional effects and $\tau\,(t) \in \mathbb{R}^n$ is the control input torque.

The mathematical model of the robot dynamics given in (1) can be reconfigured as

$$Y(q,\dot{q},\ddot{q})\,\theta = M\,(q)\,\ddot{q} + C\,(q,\dot{q})\,\dot{q} + G\,(q) + F_d\dot{q} \tag{2}$$

in which $Y\,(q,\dot{q},\ddot{q}) \in \mathbb{R}^{n\times p}$ is the regression matrix that is a function of the joint position, velocity and acceleration vectors, and $\theta \in \mathbb{R}^p$ contains constant robot model parameters. The regression matrix formulation of (2) is also written in terms of desired trajectory and its time derivatives in the following manner:

$$Y_d\,(q_d,\dot{q}_d,\ddot{q}_d)\,\theta = M\,(q_d)\,\ddot{q}_d + C\,(q_d,\dot{q}_d)\,\dot{q}_d + G\,(q_d) + F_d\dot{q}_d \tag{3}$$

https://doi.org/10.1017/S0263574721000527 Published online by Cambridge University Press

where the desired version of the regression matrix $Y_d\left(q_d, \dot{q}_d, \ddot{q}_d\right) \in \mathbb{R}^{n \times p}$ is a function of the desired joint position, velocity and acceleration vectors denoted, respectively, by $q_d\left(t\right), \dot{q}_d\left(t\right), \ddot{q}_d\left(t\right) \in \mathbb{R}^n$.

3. Control problem and error system development

The primary control objective is to design the control input torque $\tau\left(t\right)$ such that the joint position vector $q\left(t\right)$ approaches to the desired joint position vector $q_d\left(t\right)$ as time increases (i.e., the tracking control objective). In addition to the joint tracking control objective, a secondary control objective is to ensure that the entries of the position tracking error, shown with $e\left(t\right) \in \mathbb{R}^n$, remains inside a predefined bound, denoted with $\Delta_i > 0$ for each joint i, in the sense that[1]

$$\left|e_i\left(t\right)\right| < \Delta_i \; \forall t > 0. \tag{4}$$

Providing the stability of the closed-loop system by keeping all system trajectories bounded is also essential. In the subsequent development, joint position and joint velocity measurements are considered to be available. The control problem is complicated due to parametric uncertainties in the robot dynamic model (i.e., θ vector in (2) or (3) is uncertain). The desired joint position trajectory is considered to be chosen as sufficiently smooth in the sense that itself along with its first two derivatives are bounded functions of time.

In order to quantify the main control objective, the joint position tracking error $e\left(t\right) \in \mathbb{R}^n$ is defined as

$$e \triangleq q_d - q \tag{5}$$

and to present the subsequent design and the associated synthesis and analysis with only first time derivatives, a filtered error, shown with $r\left(t\right) \in \mathbb{R}^n$, is introduced

$$r \triangleq \dot{e} + \alpha e \tag{6}$$

where $\alpha \in \mathbb{R}^{n \times n}$ is a constant, positive definite, diagonal control gain matrix. To obtain the open-loop error system dynamics, the time derivative of $r\left(t\right)$ is pre-multiplied with the inertia matrix to reach

$$M\left(q\right)\dot{r} = M\left(q\right)\left(\ddot{q}_d + \alpha\dot{e}\right) + C\left(q, \dot{q}\right)\left(\dot{q}_d + \alpha e\right) - C\left(q, \dot{q}\right)r + G\left(q\right) + F_d\dot{q} - \tau \tag{7}$$

where (1) was substituted into and (6) was made use of along with the time derivative of (5). Adding and subtracting the desired robot dynamics in (3) to the right hand side of (7) deduces to

$$M\left(q\right)\dot{r} = -C\left(q, \dot{q}\right)r + \chi + Y_d\theta - \tau \tag{8}$$

with $\chi\left(q, \dot{q}, q_d, \dot{q}_d, \ddot{q}_d\right) \in \mathbb{R}^n$ being an uncertain vector defined in the following form:

$$\chi \triangleq M\left(q\right)\left(\ddot{q}_d + \alpha\dot{e}\right) + C\left(q, \dot{q}\right)\left(\dot{q}_d + \alpha e\right) + G\left(q\right) + F_d\dot{q} - Y_d\theta. \tag{9}$$

Using the boundedness properties of the the matrices forming the robot dynamics of (1), χ can be proven to be upper bounded as [25]

$$\|\chi\| \leq \rho_1\|e\| + \rho_2\|r\|. \tag{10}$$

In the above equation, the variables $\rho_1\left(\|e\|\right)$ and $\rho_2\left(\|e\|\right)$ are known, non-negative, non-decreasing functions (see Appendix A for details).

4. Control design

Based on the subsequent stability analysis, the control input torque $\tau\left(t\right)$ is designed as

$$\tau = Y_d\hat{\theta} + K_r r + K_e e + v_R \tag{11}$$

https://doi.org/10.1017/S0263574721000527 Published online by Cambridge University Press

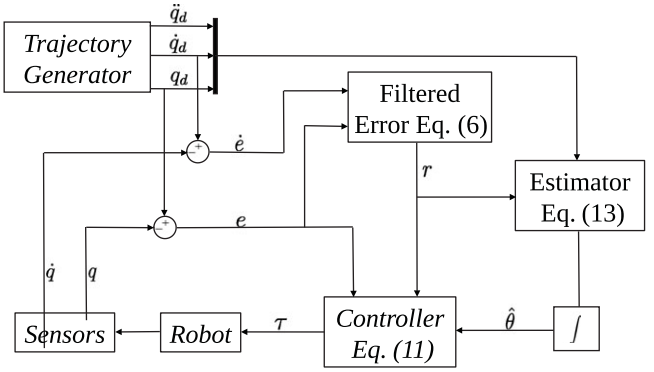

Figure 1. *Details of the controller implementation.*

where $K_r \in \mathbb{R}^{n\times n}$ is a constant, positive definite, diagonal control gain matrix, $K_e\,(e) \in \mathbb{R}^{n\times n}$ is yet to be designed tracking error dependent, positive definite, diagonal control gain matrix and $v_R\,(e, r) \in \mathbb{R}^n$ is introduced to compensate for the negative effects of χ and is designed as

$$v_R = \left(k_n \rho_1^2 + \rho_2\right) r \tag{12}$$

with $k_n \in \mathbb{R}$ being a constant, positive damping gain, and $\hat{\theta}\,(t) \in \mathbb{R}^p$ is the parameter estimation vector that is adaptively updated according to

$$\dot{\hat{\theta}} = \Gamma Y_d^T r \tag{13}$$

in which $\Gamma \in \mathbb{R}^{p\times p}$ is a constant, positive definite, diagonal adaptation gain matrix. A schematic representation of the controller implementation is presented at Fig. 1

Substituting the designed control input torque in (11) and (12) into the open-loop error system in (8) deduces the below closed-loop error system

$$M\,(q)\,\dot{r} = -C\,(q, \dot{q})\,r - K_r r - K_e e + \chi - \left(k_n \rho_1^2 + \rho_2\right) r + Y_d \tilde{\theta} \tag{14}$$

with $\tilde{\theta}\,(t) \in \mathbb{R}^p$ denoting the parameter estimation error defined as

$$\tilde{\theta} \triangleq \theta - \hat{\theta}. \tag{15}$$

Introduction of the tracking error dependent control gain matrix K_e is the main difference of this work from similar past research in the literature in the sense that the design of K_e will enable us to continue with a novel stability analysis to ensure *a priori* boundedness of the entries of the tracking error with 'user imposed' upper bounds. For this aim, two different K_e designs are proposed. The first one is designed as[2]

$$K_e = \text{diag}\left\{\frac{k_i}{\Delta_i^2 - e_i^2}\right\} \tag{16}$$

with k_i $i \in \{1, \cdots, n\}$ being constant gains, while the second one is designed as

$$K_e = \text{diag}\left\{1 + \tan^2\left(\frac{\pi}{2}\frac{e_i^2}{\Delta_i^2}\right)\right\} \tag{17}$$

with Δ_i being previously introduced in (4).

https://doi.org/10.1017/S0263574721000527 Published online by Cambridge University Press

5. Stability analysis

Despite the two tracking error dependent control gain matrix designs being fundamentally different, only the initial parts of the stability analysis differ. For both designs, the stability analysis is framed by the following theorem.

Theorem 1. *For the robot manipulator mathematical model in* (1)*, the controller in* (11) *and* (12) *along with the adaptive update law in* (13) *and the tracking error dependent control gain matrix design in either* (16) *or* (17) *ensures global asymptotic convergence of the tracking error and the filtered error to the origin and guarantees that the entries of the joint tracking error remain within a predefined bound while also proving closed-loop stability by ensuring boundedness of all the system trajectories provided that the damping gain* k_n *introduced in* (12) *is chosen sufficiently high.*

Proof. For the tracking error dependent diagonal controller gain matrix design in (16), the analysis is initiated by defining the barrier Lyapunov function $V_l\left(r, e, \tilde{\theta}\right) \in \mathbb{R}$ as

$$V_l \triangleq \frac{1}{2} r^T M\left(q\right) r + \sum_{i=1}^{n} \frac{k_i}{2} \ln\left(\frac{\Delta_i^2}{\Delta_i^2 - e_i^2}\right) + \frac{1}{2} \tilde{\theta}^T \Gamma^{-1} \tilde{\theta} \tag{18}$$

which is positive definite and radially unbounded provided that the initial values of the entries of the joint tracking error satisfies $|e_i\left(0\right)| < \Delta_i$ for all $i \in \{1, \cdots, n\}$.

Taking the time derivative of (18) yields

$$\dot{V}_l = r^T M\left(q\right) \dot{r} + \frac{1}{2} r^T \dot{M}\left(q\right) r + \sum_{i=1}^{n} k_i \frac{e_i \dot{e}_i}{\Delta_i^2 - e_i^2} + \tilde{\theta}^T \Gamma^{-1} \dot{\tilde{\theta}} \tag{19}$$

in which

$$\sum_{i=1}^{n} k_i \frac{e_i \dot{e}_i}{\Delta_i^2 - e_i^2} = e^T K_e \dot{e} \tag{20}$$

in view of the diagonal structure of K_e in (16). Substituting the closed-loop error system in (14) for r dynamics, (20) and (6) for e dynamics, the time derivative of (15) along with (13) for $\tilde{\theta}$ dynamics into (19) deduces

$$\begin{aligned} \dot{V}_l \;=\; & r^T \left[-C\left(q, \dot{q}\right) r - K_r r - K_e e + \chi - \left(k_n \rho_1^2 + \rho_2\right) r + Y_d \tilde{\theta}\right] \\ & + \frac{1}{2} r^T \dot{M}\left(q\right) r + e^T K_e \left(-\alpha e + r\right) - \tilde{\theta}^T Y_d^T r. \end{aligned} \tag{21}$$

At the right-hand side of (21), making use of the skew–symmetry relationship (i.e., $\xi^T \left(\dot{M} - 2C\right) \xi = 0 \; \forall \xi \in \mathbb{R}^n$), upper bounding χ with (10) and then cancelling common terms give

$$\dot{V}_l \leq -r^T K_r r - e^T K_e \alpha e + \left[\rho_1 \|e\| \|r\| - k_n \rho_1^2 \|r\|^2\right] \tag{22}$$

in which for the square bracketed term [26]

$$\rho_1 \|e\| \|r\| - k_n \rho_1^2 \|r\|^2 \leq \frac{1}{4k_n} \|e\|^2 \tag{23}$$

can be used to further obtain an upper bound as

$$\dot{V}_l \leq -\lambda_{\min}\{K_r\} \|r\|^2 - \left(\lambda_{\min}\{K_e \alpha\} - \frac{1}{4k_n}\right) \|e\|^2. \tag{24}$$

https://doi.org/10.1017/S0263574721000527 Published online by Cambridge University Press

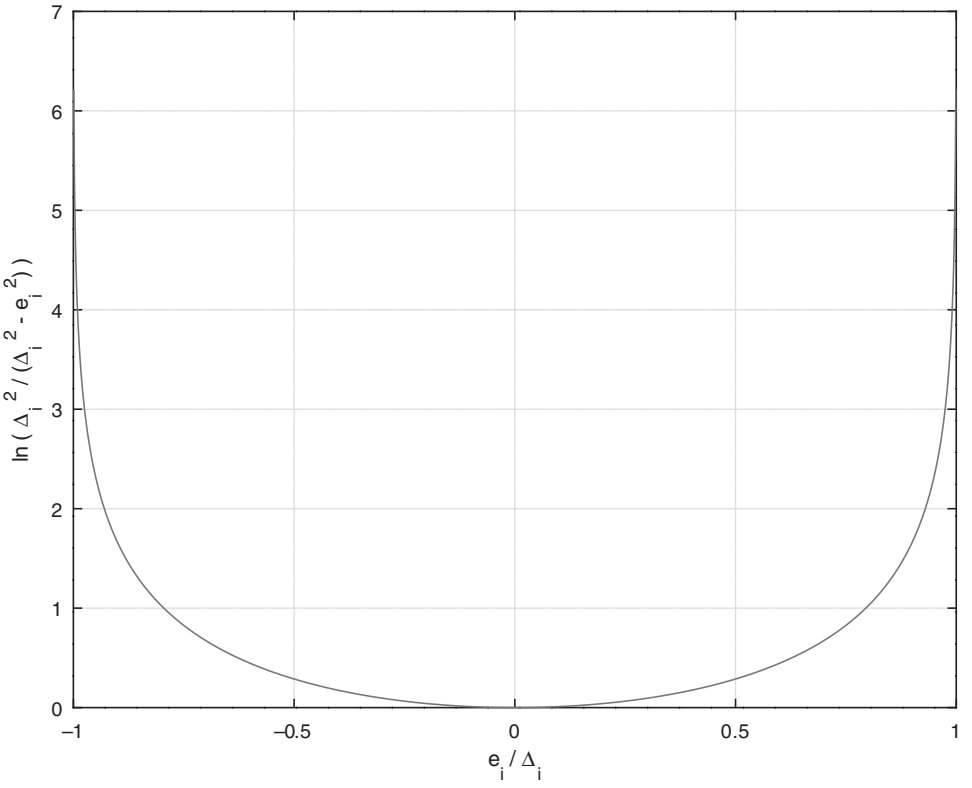

Figure 2. *The "logarithmic" component of $V_l(t)$.*

After defining the combined error vector $x \triangleq \left[r^T \; e^T \right]^T \in \mathbb{R}^{2n}$ and positive constant $\beta \in \mathbb{R}$ as

$$\beta \triangleq \min \left\{ \lambda_{\min}\{K_r\}, \lambda_{\min}\{K_e \alpha\} - \frac{1}{4k_n} \right\} \tag{25}$$

following upper bound can be obtained for the right-hand side of (24)

$$\dot{V}_l \leq -\beta \|x\|^2 \tag{26}$$

provided that k_n is chosen sufficiently high.

From the structures of (18) and (26), V_l is proven to be bounded and decreasing. Thus $r(t)$, $e(t)$, $\tilde{\theta}(t) \in \mathcal{L}_\infty$ and are also decreasing. By utilising the boundedness of the above terms along with the boundedness of the desired trajectory and its time derivatives, $\dot{e}(t)$, $\dot{r}(t) \in \mathcal{L}_\infty$ can be proven from (6) and (14), respectively. It can straightforwardly be shown that the remaining terms can be ensured to be bounded as well. After integrating (26) on time from initial time to infinity, $x(t)$ is proven to be square integrable and thus $r(t)$, $e(t) \in \mathcal{L}_2$. Since $x(t) \in \mathcal{L}_2 \cap \mathcal{L}_\infty$ and $x(t) \in \mathcal{L}_\infty$, from Barbalat's Lemma [27, 28] $x(t) \to 0$ as $t \to \infty$ is proven.

We would like to note that due to the structure of $V_l(t)$ given in (18) and the negativeness of $\dot{V}_l(t)$ of (26), the positive function V_l is decreasing with respect to time. And since the first and third terms of $V_l(t)$ are quadratic with respect to $r(t)$ and $\tilde{\theta}$, respectively, the term in the middle, as can be seen from Fig. 2, should be also decreasing with time . When the initial error signal $e_i(0)$ is selected inside the region $(-\Delta_i, +\Delta_i)$, the tracking error signal will always stay inside this region and converge to zero asymptotically. Therefore the singularities in (16) are always avoided.

https://doi.org/10.1017/S0263574721000527 Published online by Cambridge University Press

For the tracking error dependent diagonal controller gain matrix design in (17), the analysis is initiated by defining a similar barrier Lyapunov function, denoted by $V_t\left(r, e, \tilde{\theta}\right) \in \mathbb{R}$, as

$$V_t \triangleq \frac{1}{2} r^T M\left(q\right) r + \sum_{i=1}^{n} \frac{\Delta_i^2}{\pi} \tan\left(\frac{\pi}{2} \frac{e_i^2}{\Delta_i^2}\right) + \frac{1}{2} \tilde{\theta}^T \Gamma^{-1} \tilde{\theta} \tag{27}$$

where only the second term is different than the corresponding term in (18). It is noted that $V_t\left(r, e, \tilde{\theta}\right)$ is positive definite and radially unbounded provided that the initial values of the entries of the joint tracking error satisfy $|e_i\left(0\right)| < \Delta_i$ for all $i \in \{1, \cdots, n\}$.

The time derivative of (27) is obtained as

$$\dot{V}_t = r^T M\left(q\right) \dot{r} + \frac{1}{2} r^T \dot{M}\left(q\right) r + \sum_{i=1}^{n} e_i \dot{e}_i \left(1 + \tan^2\left(\frac{\pi}{2} \frac{e_i^2}{\Delta_i^2}\right)\right) + \tilde{\theta}^T \Gamma^{-1} \dot{\tilde{\theta}} \tag{28}$$

where, in view of the diagonal structure of K_e design in (17), the third term can be reformulated as

$$\sum_{i=1}^{n} e_i \dot{e}_i \left(1 + \tan^2\left(\frac{\pi}{2} \frac{e_i^2}{\Delta_i^2}\right)\right) = e^T K_e \dot{e}. \tag{29}$$

A closer look at the structure of (28) in view of (29) reveals the fact that it is the same as (19) used with (20), thus the rest of the analysis is same as the previous part. □

Despite obtaining the same result for both choices of tracking error dependent control gain matrices, due to the differences in their designs in (16) and (17), the resulting β values may be different. For the design in (16), $\lambda_{\min}\{K_e \alpha\}$ is equal to $\min\{\frac{k_i \alpha_i}{\Delta_i^2 - e_i^2}\}$ over $i \in \{1, \cdots, n\}$, which can conservatively be obtained as $\frac{\min\{k_i \alpha_i\}}{\max\{\Delta_i^2\}}$. On the other hand, for the design in (17), $\lambda_{\min}\{K_e \alpha\}$ is equal to $\min\{\alpha_i \left(1 + \tan^2\left(\frac{\pi}{2} \frac{e_i^2}{\Delta_i^2}\right)\right)\}$ over $i \in \{1, \cdots, n\}$ which, after noting that the $\tan^2(\cdot)$ term being non-negative, can be conservatively obtained as $\min\{\alpha_i\}$.

6. Numerical studies

Numerical simulations on the model of a two-link planar robot manipulator were performed to demonstrate the viability of the proposed adaptive control strategy. The model of the robot manipulator has the following form:

$$\begin{aligned} \begin{bmatrix} \tau_1 \\ \tau_2 \end{bmatrix} &= \begin{bmatrix} \theta_1 + 2\theta_3 \cos\left(q_2\right) & \theta_2 + \theta_3 \cos\left(q_2\right) \\ \theta_2 + \theta_3 \cos\left(q_2\right) & \theta_2 \end{bmatrix} \begin{bmatrix} \ddot{q}_1 \\ \ddot{q}_2 \end{bmatrix} \\ &+ \begin{bmatrix} -\theta_3 \dot{q}_2 \sin\left(q_2\right) & -\theta_3 \left(\dot{q}_1 + \dot{q}_2\right) \sin\left(q_2\right) \\ \theta_3 \dot{q}_1 \sin\left(q_2\right) & 0 \end{bmatrix} \begin{bmatrix} \dot{q}_1 \\ \dot{q}_2 \end{bmatrix} \\ &+ \begin{bmatrix} \theta_4 & 0 \\ 0 & \theta_5 \end{bmatrix} \begin{bmatrix} \dot{q}_1 \\ \dot{q}_2 \end{bmatrix}. \end{aligned} \tag{30}$$

In the above model, $\theta_1, \theta_2, \theta_3$ are model parameters that depend on masses and lengths of the links of the robot manipulator, while θ_4 and θ_5 are viscous friction parameters. In commensurate with the analysis above, these model parameters are considered to be uncertain and thus are not available for the control design. For the numerical simulations to be realistic, the control input torque values were saturated at ± 10 [Nm]. The robot model and the dynamical parameters are obtained from the IMI robot [29], where a picture and a schematic representation of the robot is given in Fig. 3.

https://doi.org/10.1017/S0263574721000527 Published online by Cambridge University Press

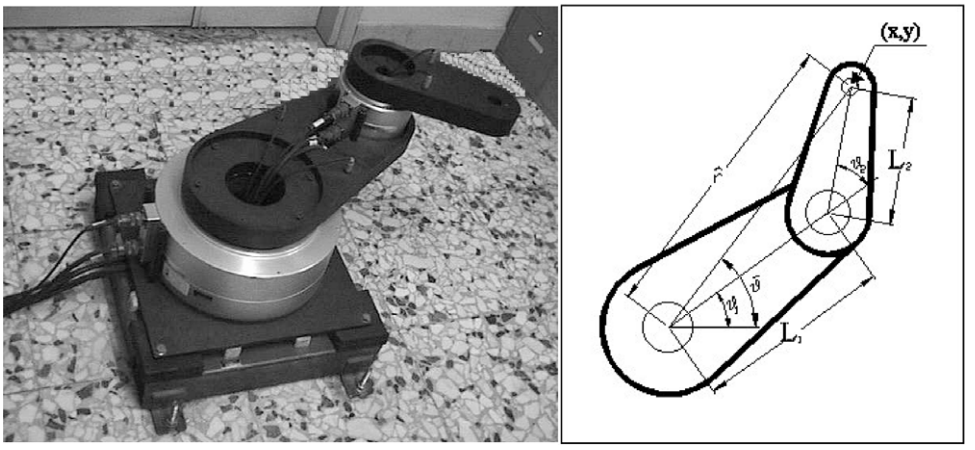

Figure 3. *Two-link planar IMI robot.*

In the numerical simulations, the following desired joint trajectory was used:

$$q_d(t) = \begin{bmatrix} 0.7 \sin(t) \left(1 - e^{-0.3t^3}\right) \\ 1.2 \sin(t) \left(1 - e^{-0.3t^3}\right) \end{bmatrix} [\text{rad}]. \tag{31}$$

The joints of the robot manipulator were initially positioned such as the initial value of the tracking error for both joints were 2.9°. The initial values of the parameter estimation vector, $\hat{\theta}(0)$, were set to zero and the actuators are assumed to be driven in torque mode.

The results of three sets of numerical simulations are presented with Δ_i chosen as 3°, 5° and 10°, respectively, for each joint of the robot manipulator. The control and adaptation gain matrices were tuned via trial and error in the sense that initially, higher gains were chosen and they are decreased until a satisfactory joint position tracking performance was obtained. The controller and adaptation gains, for all three numerical simulations, were selected as

$$\alpha = 2I_2\,,\ K_r = 50I_2\,,\ k_1 = k_2 = 2 \tag{32}$$

$$\Gamma = \text{diag}\{50,\ 0.8,\ 1.255,\ 100.6,\ 40.2\}. \tag{33}$$

The results of the simulation studies for different values of position constraints are presented in Figs., 4, 5 and 7, respectively. For each simulation the joint tracking errors, the parameter estimate updates and the control input torque are plotted with respect to time. For the comparison of the initial controller effort, Table 1 presents the $\mathcal{L}_2$ norms of the controller efforts for each simulation where we can observe that the overall control effort decreases as the position constraint on the joints are changed from 3° to 10°. The $\mathcal{L}_2$ norm of the controller efforts at steady state are presented at Table 2 from which it can be observed that there is no significant change on the amount of controller efforts when the system reaches steady state. Finally from the dynamical parameter estimate plots given Figs. 4, 5 and 7, we can conclude that increasing the position constraint on the joint trajectories increases the time for the convergence of the parameter estimates (i.e., delays the parameter convergence process).

7. Experimental validations

In order to illustrate the feasibility and performance of the proposed position constrained adaptive controller, experimental studies are performed on a two-link direct-drive planar robot manipulator assembled in Gebze Technical University, Control Applications and Robotics Laboratory. The dynamical model of the robot is similar to (30) with the values of θ_i, $i = 1...5$ being uncertain. The links of the manipulator are constructed from aluminium with link lengths of 16 cm for the first link and 6.5 cm for

https://doi.org/10.1017/S0263574721000527 Published online by Cambridge University Press

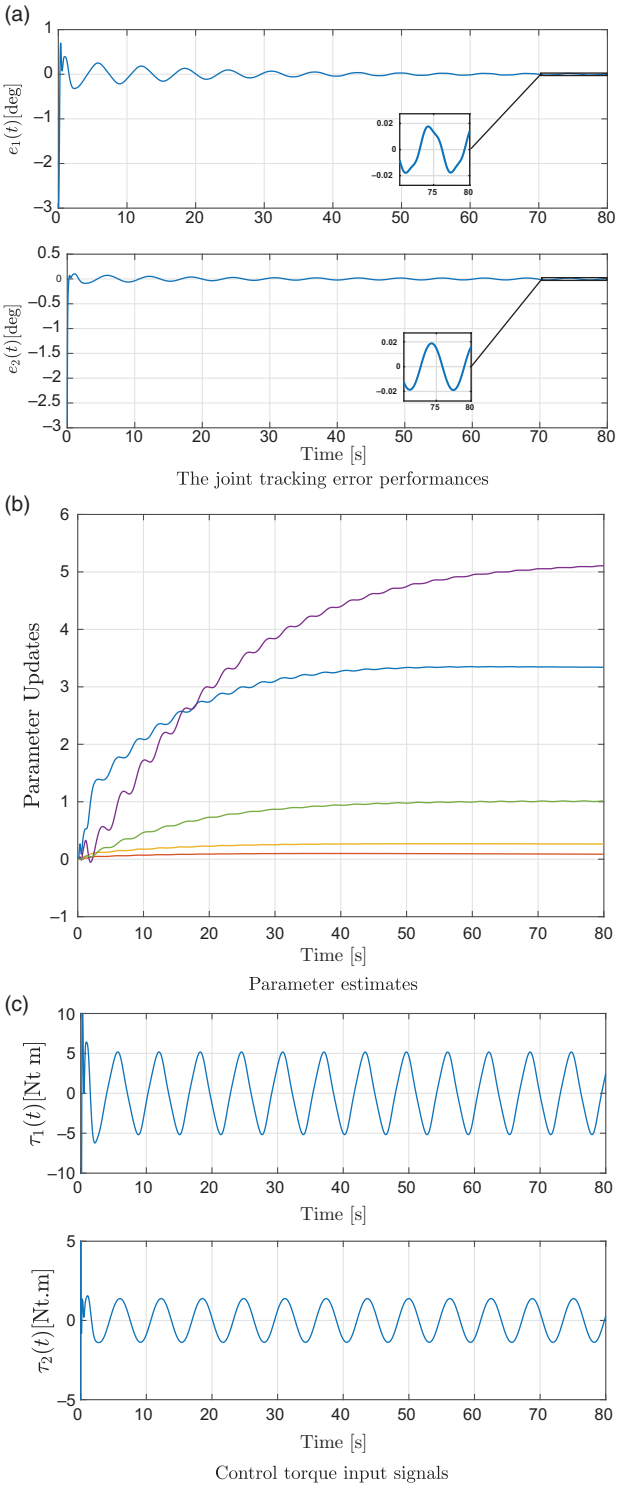

Figure 4. *Simulation results when the position constraint on joint angles is 3°.*

https://doi.org/10.1017/S0263574721000527 Published online by Cambridge University Press

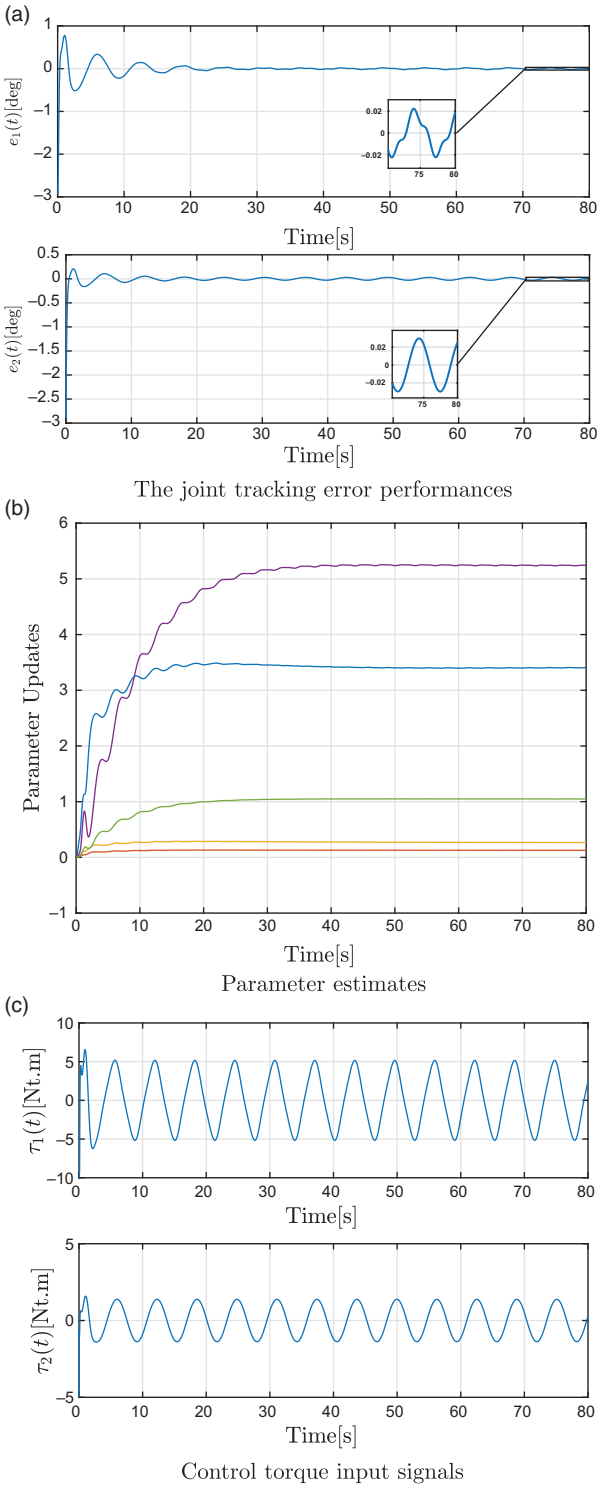

Figure 5. *Simulation results when the position constraint on joint angles is 5°.*

https://doi.org/10.1017/S0263574721000527 Published online by Cambridge University Press

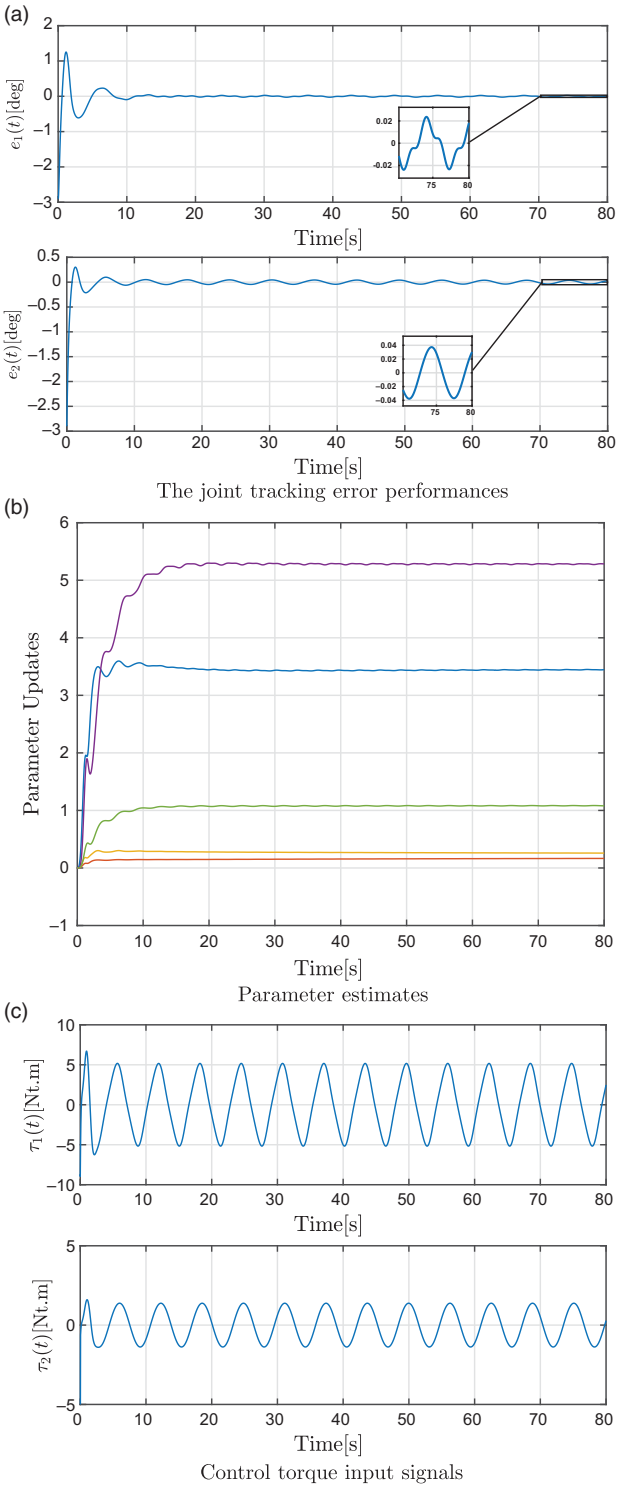

Figure 6. *Simulation results when the position constraint on joint angles is 10°.*

https://doi.org/10.1017/S0263574721000527 Published online by Cambridge University Press

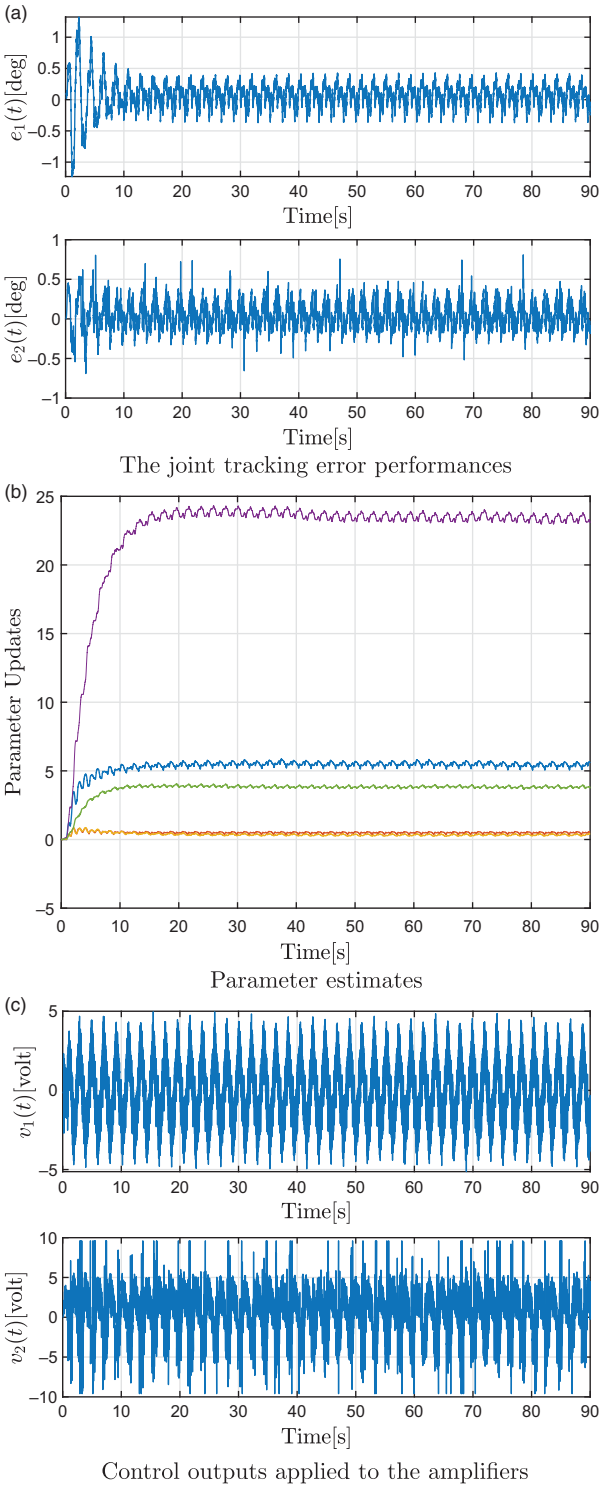

Figure 7. *Experimental results when the position constraint on joint angles is 10°.*

https://doi.org/10.1017/S0263574721000527 Published online by Cambridge University Press

Table 1. *$\mathcal{L}_2$ norm of the torque inputs for $0 \leq t \leq 20[s]$.*

	$\Delta_i = 3$ [deg]	$\Delta_i = 5$ [deg]	$\Delta_i = 10$ [deg]
$\left\{\int_0^{20} \tau_1(t)dt\right\}^{1/2}$	540.7435	523.7784	514.0927
$\left\{\int_0^{20} \tau_2(t)dt\right\}^{1/2}$	150.1854	143.568	141.5573

Table 2. *$\mathcal{L}_2$ norm of the torque inputs for $70 \leq t \leq 80[s]$.*

	$\Delta_i = 3$ [deg]	$\Delta_i = 5$ [deg]	$\Delta_i = 10$ [deg]
$\left\{\int_{70}^{80} \tau_1(t)dt\right\}^{1/2}$	338.3291	338.3548	338.3563
$\left\{\int_{70}^{80} \tau_2(t)dt\right\}^{1/2}$	95.3373	95.3455	95.3514

the second link. Link 1 is actuated via a SanyoDenko dc motor equipped with a 4096 counts/revolution encoder and second link is actuated via a Escap dc motor with an encoder having 2048 counts/revolution. Each motor is actuated via an in-house build linear amplifier having unity gain.

For the experimental studies, the position tracking error constraint was set to $10[deg]$ the same desired trajectory used in the simulation studies were applied (i.e., Eq. (31)), the initial values of the parameter estimates were set to zero and the controller,and adaptation gains were tuned until the best error tracking and parameter adaptations were obtained. The selected control and adaptation gains were as follows:

$$\alpha = diag\{10, 20\}, \quad k_e = diag\{12, 24\},$$
$$K_r = diag\{180, 50\}$$
and
$$\Gamma = diag\{6, 0.5, 0.4, 24, 4.5\}$$

The results of the experiments are presented in Fig. 7, where the top two sub-figures are the tracking error performances, the sub-figure in the middle is the parameter estimations and the bottom two sub-figures are the corresponding voltage outputs of the current amplifiers (representing the control torque inputs). As can be seen from Fig. 7, after around 20 s, the parameter estimates converge to some values and the tracking error performances for link 1 and 2 converge to values below $\pm 0.5[deg]$.

8. Conclusion

In this work, we have presented the design and the corresponding analysis of two different types of full-state feedback, desired model-based, joint position constrained, robot controllers using barrier Lyapunov functions. The proposed controllers ensure that the position tracking error of the robot joints remain inside a predefined value and eventually converge to zero when the initial tracking error starts inside this predefined region, despite the presence of uncertainties in the parameters of robot dynamics. To our best knowledge, the proposed controller methodology is the first approach that fuses the use of BLF design with the desired model-based compensation procedure. The use of the desired trajectory signal as opposed to the actual state variables enables a smoother controller output and is less exposed to sensory noise. Extensive numerical simulations are performed to illustrate the performance of the proposed methods for three different values of constraints on joint positions. Experimental studies performed on a two-link direct-drive robot arm is also presented in order to illustrate the feasibility of the proposed controller. Future work will concentrate on output feedback version of the proposed method and extending this result to task space control of robotic manipulators.

https://doi.org/10.1017/S0263574721000527 Published online by Cambridge University Press

Notes

1 In this paper, subscript *i* of a diagonal matrix or a column vector denote the *i*th diagonal entry of the matrix or the *i*th entry of the vector, respectively.
2 The notation diag{·} denotes a diagonal matrix with its diagonal entries being the ones in the braces.

References

[1] K. Merckaert, B. Vanderborght, M. Nicotra and E. Garone, "Constrained Control of Robotic Manipulators Using the Explicit Reference Governor," *2018 IEEE/RSJ International Conference on Intelligent Robots and Systems (IROS)* (2018) pp. 5155–5162.
[2] K. B. Ngo, R. Mahony and Z. P. Jiang, "Integrator Backstepping Using Barrier Functions for Systems with Multiple State Constraints," *Proceedings of the 44th Conference on Decision and Control*, Seville, Spain (2005) pp. 8306–8312.
[3] K. P. Tee, S. S. Ge and E. H. Tay, "Barrier lyapunov functions for the control of output-constrained nonlinear systems," *Automatica* **45**(4), 918–927 (2009).
[4] K. P. Tee, B. Ren and S. S. Ge, "Control of nonlinear systems with time-varying output constraints," *Automatica* **47**(11), 2511–2516 (2011).
[5] Y. J. Liu and S. C. Tong, "Barrier Lyapunov functions-based adaptive control for a class of nonlinear pure-feedback systems with full state constraints," *Automatica* **64**, 70–75 (2016).
[6] C. Wang, Y. Wu and J. Yu, "Barrier Lyapunov functions-based adaptive control for nonlinear pure-feedback systems with time-varying full state constraints," *Int. J. Cont. Automat. Syst.* **15**(6), 2714–2722 (2017).
[7] A. LAfflitto, "Barrier Lyapunov functions and constrained model reference adaptive control," *IEEE Cont. Syst. Lett.* **2**(3), 441–446 (2018).
[8] G. Buizza Avanzini, A. Zanchettin and P Rocco, "Constrained model predictive control for mobile robotic manipulators", *Robotica*, **36**, 19–38 (2018).
[9] J. Kabziński, P. Mosiołek and M. Jastrzkbski, "Adaptive Position Tracking with Hard Constraints – Barrier Lyapunov Functions Approach," **In:** *Advanced Control of Electrical Drives and Power Electronic Converters* (J. Kabziński, ed.) (Springer, Cham, Switzerland, 2017) pp. 27–52.
[10] Z. Doulgeri and O. Zoidi, "Prescribed Performance Regulation for Robot manipulators," *Proceedings of International IFAC Symposium on Robot Control* (2009) pp. 721–726.
[11] Z. Doulgeri and Y. Karayiannidis, "PID Type Robot Joint Position Regulation with Prescribed Performance Guaranties," *Proceedings of IEEE International Conference on Robotics and Automation* (2010) pp. 4137–4142.
[12] Y. Karayiannidis and Z. Doulgeri, "Model-free robot joint position regulation and tracking with prescribed performance guarantees," *Robot. Autonom. Syst.* **60**, 214–226 (2012).
[13] Y. Karayiannidis and Z. Doulgeri, "Regressor-free prescribed performance robot tracking," *Robotica* **31**, 1229–1238 (2013).
[14] Y. Karayiannidis, D. Papageorgiou and Z. Doulgeri, "A model–free controller for guaranteed prescribed performance tracking of both robot joint positions and velocities," *IEEE Robot. Automat. Lett.* **1**(1), 267–273 (2016).
[15] C. Hackl and R. Kennel, "Position Funnel Control for Rigid Revolute Joint Robotic Manipulators with Known Inertia Matrix," *Mediterranean Conference on Control and Automation* (2012) pp. 615–620.
[16] Z. Doulgeri and L. Droukas, "Robot Task Space PID Type Regulation with Prescribed Performance Guaranties," *Proceedings of IEEE/RSJ International Conference on Intelligent Robots Systems*, Taipei, Taiwan (2010) pp. 1644–1649.
[17] D. Papageorgiou, A. Atawnih and Z. Doulgeri, "A Passivity Based Control Signal Guaranteeing Joint Limit Avoidance in Redundant Robots," *Mediterranean Conference on Control and Automation*, Athens, Greece (2016) pp. 569–574.
[18] Z. Doulgeri and P. Karalis, "A Prescribed Performance Referential Control for Human-Like Reaching Movement of Redundant Arms," *Proceedings of International IFAC Symposium on Robot Control* (2012) pp. 295–300.
[19] C. Bechlioulis, Z. Doulgeri and G. Rovithakis, "Guaranteeing prescribed performance and contact maintenance via an approximation free robot force/position controller," *Automatica* **48**(2), 360–365 (2012).
[20] C. P. Bechlioulis, Z. Doulgeri and G. A. Rovithakis, "Neuro-adaptive force/position control with prescribed performance and guaranteed contact maintenance," *IEEE Trans. Neural Netw.* **21**(12), 1857–1868 (2010).
[21] J. J. B. M. Ahanda, J. B. Mbede, A. Melingui and B. E. Zob, "Robust adaptive command filtered control of a robotic manipulator with uncertain dynamic and joint space constraints," *Robotica* **35**, 767–786 (2018).
[22] J. Xia, Y. Zhang, C. Yang, M. Wang and A. Annamalai, "An improved adaptive online neural control for robot manipulator systems using integral Barrier Lyapunov functions," *Int. J. Syst. Sci.* **50**(3), 638–651 (2019).
[23] J. Villalobos-Chin and V. Santibáñez, "An adaptive regressor-free Fourier series-based tracking controller for robot manipulators: Theory and experimental evaluation", *Robotica*, 1–16 (2021). doi:10.1017/S0263574721000084.
[24] S. Khorashadizadeh and M. M. Fateh, "Uncertainty estimation in robust tracking control of robot manipulators using the Fourier series expansion", *Robotica* **35**, 310–336 (2017).
[25] F. L. Lewis, D. M. Dawson and C. T. Abdallah, *Robot Manipulator Control: Theory and Practice* (Marcel Dekker, Inc., New York, NY, USA, 2004).

[26] P. Kokotovic, "The joy of feedback: Nonlinear and adaptive," *IEEE Cont. Syst. Mag.* **12**(3), 7–17 (1992).
[27] M. Krstic, I. Kanellakopoulos and P. V. Kokotovic, *Nonlinear and Adaptive Control Design* (Wiley, New York, NY, USA, 1995). ISBN: 988-0-471-12732-1.
[28] H. K. Khalil, *Nonlinear Systems*, 3rd Edition (Prentice Hall, New York, NY, USA, 2002).
[29] *Direct Drive Manipulator Research and Development Package Operations Manual* (Integrated Motion Inc., Berkeley, CA, 1992).

Appendix A

The auxiliary term χ given in (10) can be explicitly written as

$$\begin{aligned}\chi \triangleq & M(q)\left(\ddot{q}_d + \alpha\dot{e}\right) + C(q,\dot{q})\left(\dot{q}_d + \alpha e\right) + G(q) + F_d\dot{q} \\ & - M(q_d)\ddot{q}_d - C(q_d,\dot{q}_d)\dot{q}_d - G(q_d) - F_d\dot{q}_d\end{aligned} \tag{34}$$

where (3) has been applied. Similar to [25] (Chapter 6, Eq. 6.2-9) this term can be upper bounded as

$$\|\chi\| \leq \zeta_1 \|e\| + \zeta_2 \|e\|^2 + \zeta_3 \|r\| + \zeta_4 \|r\| \|e\| \tag{35}$$

where $\zeta_i, i = 1, 2, 3, 4$ are positive bounding constants that depend on the desired trajectory and physical parameters (i.e., link mass, link length, friction coefficients, etc.). After some mathematical manipulations (35), the upper bound can be reformulated as follows:

$$\|\chi\| \leq (\zeta_1 + \zeta_2 \|e\|) \|e\| + (\zeta_3 + \zeta_4 \|e\|) \|r\| . \tag{36}$$

It is straightforward when the bounding functions $\rho_1(e)$, and $\rho_2(e)$ are selected as

$$\begin{aligned}\rho_1(e) &= \zeta_1 + \zeta_2 \|e\| \\ \rho_2(e) &= \zeta_3 + \zeta_4 \|e\|\end{aligned} \tag{37}$$

bound given in (10) is satisfied.

Cite this article: S. Gul, E. Zergeroglu, E. Tatlicioglu and M. V. Kilinc (2022). "Desired Model Compensation-Based Position Constrained Control of Robotic Manipulators", Robotica **40**, 279–293. https://doi.org/10.1017/S0263574721000527